

# Lab in a Tube: Ultrasensitive Detection of MicroRNAs at the Single-Cell Level and in Breast Cancer Patients Using Quadratic Isothermal Amplification

Ruixue Duan,<sup>†,⊥</sup> Xiaolei Zuo,<sup>‡,⊥</sup> Shutao Wang,<sup>§,⊥</sup> Xiyun Quan,<sup>||</sup> Dongliang Chen,<sup>||</sup> Zhifei Chen,<sup>†</sup> Lei Jiang,<sup>§</sup> Chunhai Fan,<sup>‡</sup> and Fan Xia<sup>\*,†</sup>

<sup>†</sup>School of Chemistry and Chemical Engineering, Huazhong University of Science and Technology, Wuhan 430074, China

<sup>‡</sup>Laboratory of Physical Biology, Shanghai Institute of Applied Physics, Chinese Academy of Sciences, Shanghai 201800, China

<sup>§</sup>Beijing National Laboratory for Molecular Sciences (BNLMS), Key Laboratory of Organic Solids, Institute of Chemistry, Chinese Academy of Sciences, Beijing 100190, China

<sup>||</sup>The Pathology Department of Zhuzhou No. 1 Hospital, Hunan 412000, China

## Supporting Information

**ABSTRACT:** Through rational design of a functional molecular probe with high sequence specificity that takes advantage of sensitive isothermal amplification with simple operation, we developed a one-pot hairpin-mediated quadratic enzymatic amplification strategy for microRNA (miRNA) detection. Our method exhibits ultrahigh sensitivity toward miR-21 with detection limits of 10 fM at 37 °C and 1 aM at 4 °C, which corresponds to nine strands of miR-21 in a 15 μL sample, and it is capable of distinguishing among miRNA family members. More importantly, the proposed approach is also sensitive and selective when applied to crude extractions from MCF-7 and PC3 cell lines and even patient tissues from intraductal carcinoma and invasive ductal carcinoma of the breast.

Accurate and quantitative analysis of microRNA (miRNA) expression has become imperative for further understanding the biological functions of miRNAs, early diagnosis of disease, and discovery of new anticancer drugs.<sup>1–5</sup> Northern-blotting technology<sup>6</sup> and microarrays<sup>7,8</sup> are most widely used for miRNA quantification. However, great progress in improving the sensitivity and specificity has been hindered by the small size, sequence homology among family members, and low abundance of miRNAs. Recently, various amplification strategies have been developed for miRNA detection, such as the modified invader assay,<sup>9</sup> ribozyme amplification,<sup>10</sup> real-time polymerase chain reaction (RT-PCR),<sup>11–13</sup> and nanoparticle-amplified approaches.<sup>14,15</sup> Among these methods, RT-PCR has attracted much attention because of its high sensitivity and practicality. Nevertheless, RT-PCR requires precise control of the temperature cycling to achieve amplification, which imposes instrumentation constraints on its wider and more versatile applications. In addition, the short length of miRNAs makes the PCR design very sophisticated and decreases the assay reliability, especially in some complex clinical samples with PCR inhibitors and interferents.<sup>11</sup>

Molecular beacon (MB)-assisted isothermal oligonucleotide amplification, with its inherent stability, specificity, and

simplicity, has recently emerged as a potential amplification technique for rapid and cost-effective detection of oligonucleotides.<sup>16–25</sup> Unfortunately, this method is limited by its unsatisfactory sensitivity or the nicking endonuclease recognition site contained in the target oligonucleotides.<sup>19–25</sup> In the present work, we developed an ultrasensitive one-pot miRNA detection scheme that uses hairpin-mediated quadratic enzymatic amplification (HQEA) to circumvent the aforementioned limitations in miRNA detection. More importantly, our method is suitable for the direct detection of miRNAs in crude cellular extracts of cancer cells and even patient tissues.

The first step of our amplification strategy is initiated by the hybridization of the target miRNA with the loop region of the MB probe, leading to a conformational change in which the MB stem opens, resulting in emission of the fluorescent signal. Next, an engaging primer anneals with the open stem and allows polymerization induced by Bst polymerase, which displaces the target miRNA and synthesizes a DNA duplex according to the MB probe. As a result, the beacon is still activated and emits a fluorescence signal, whereas the displaced miRNA is free to bind to another beacon, initiating a new cycle. With each reaction cycle, the miRNA target is regenerated, another beacon is activated, and a duplex beacon is formed (Figure 1 right).

The duplex beacon produced from the first cycle generates a nicking enzyme recognition site. In the absence of target, the beacon is inactive, and the recognition sequence remains as a single strand, which is an unsuitable substrate for the nicking endonuclease. Only when the duplex beacon is produced is the DNA recognition sequence a suitable substrate for the nicking endonuclease. Following nicking of the beacon, the 5' end of the beacon labeled by phosphorothioate is cleaved and dissociated from the MB probe, exposing the recognition site of lambda exonuclease, which can catalyze the stepwise removal of mononucleotides from 5'-hydroxyl termini of duplex DNAs. With each reaction, a new single-stranded DNA (ssDNA) complementary to the MB is synthesized. It is the newly

**Received:** November 29, 2012

**Published:** February 27, 2013

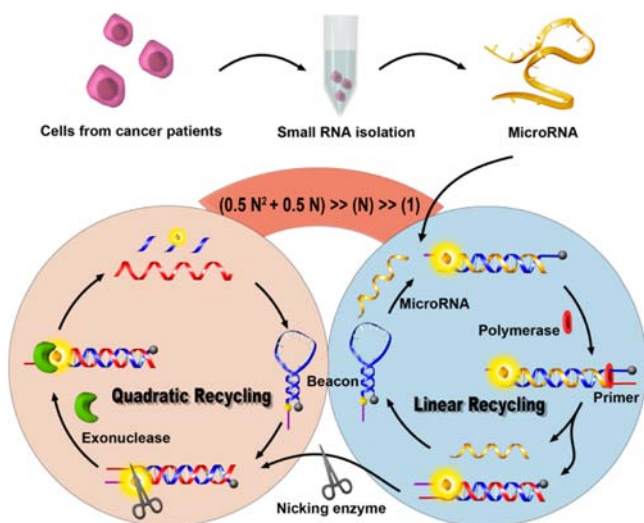


**Figure 1.** Schematic illustration of the HQEA strategy based on a *Bst* polymerase-induced strand-displacement reaction and a lambda exonuclease-aided recycling reaction.

synthesized ssDNA that acts as another target to trigger the next reaction and initiate the second recycle. The newly synthesized DNA perfectly matched with the beacon binds to another beacon and activates it, forming a new nicking enzyme recognition site. With each digestion cycle, a new DNA target is regenerated, which can activate an additional beacon. Thus, once initiated, the polymerase regenerates the miRNA target in the first amplification cycle, and the nicking enzyme and lambda exonuclease produce multiple copies of the newly recycled target DNA in the second cycle. This enables multiple beacons to be activated in a series of cyclic chain reactions, enhancing the fluorescence signal (Figure 1 left).

The quadratic amplification of the reaction is best characterized not only by recycled target miRNA triggered by *Bst* polymerase but also by another recycled ssDNA target produced during the first recycling reaction. For the proof-of-concept experiment, we selected miR-21 as our initial target [Table S1 in the Supporting Information (SI)]. The progress of the reaction was monitored via the fluorescence emitted from duplex MBs and digested MBs (Figure 2a). It is clear that this strategy is dependent on the polymerase, as no signal increase was observed when it was omitted from the reaction. Furthermore, the signal amplification obviously relies on the

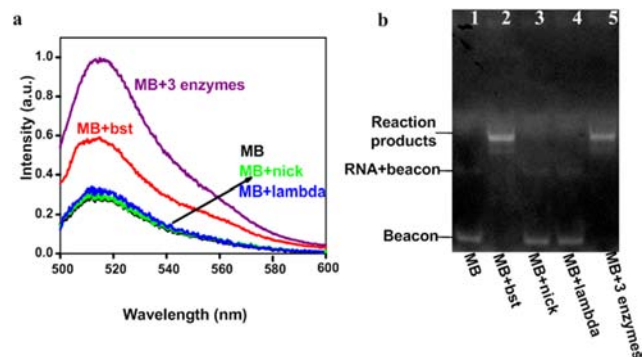


**Figure 2.** Effects of different enzymes on the amplification reaction within 40 min, as analyzed by (a) fluorescence emission and (b) PAGE.

nicking endonuclease and lambda exonuclease, since the fluorescence signal substantially increased upon addition of the three enzymes simultaneously.

The above results were further conformed by polyacrylamide gel electrophoresis (PAGE) (Figure 2b), which showed that only polymerase can start the circular strand-displacement reaction and produce duplex MBs. As expected, when nicking endonuclease or lambda exonuclease alone was added, no duplex MB was produced. It is worth noting that in the presence of all three enzymes, the duplex DNA content decreased compared with that in the presence of only polymerase because lambda exonuclease digests one of the strands of the duplex DNA. Additionally, at the beginning of the reaction, the rate is expected to increase with time because the reaction of the second recycle is more efficient than that of the first recycle (Figures S4 and S7 in the SI). However, with the decrease of the remaining concentration of MBs in the reaction buffer, the rate should decrease and finally tend to zero. It should be pointed out that the sequence recognized by endonuclease at the 5' terminus should not hybridize to the other end of free MBs; otherwise nonspecific nicking will occur, decreasing the sensitivity (Figure S2).

We further investigated the effects of temperature on the traditional MB method, *Bst* polymerase-induced strand-displacement amplification, and the HQEA approach (Figures 3, S3–S5, and S9–S15). The results demonstrate that the

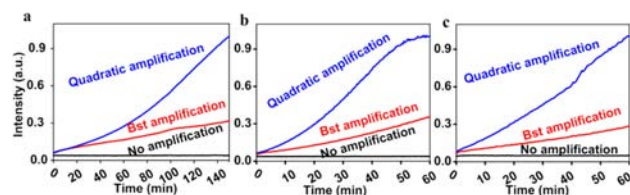


**Figure 3.** Time-dependent fluorescence changes at (a) 25, (b) 37, and (c) 50 °C using quadratic amplification (blue), *Bst*-induced amplification (red), and the traditional MB method (black).

amplification mode of our proposed technology is quadratic, which is more efficient than the other two methods at 25, 37, or 50 °C (Figures S3a, S4a, and S5a). At the beginning of the quadratic reaction, the rate is limited by the low concentration of duplex beacons, one of its reactants produced from the first recycle, and it is slightly higher than that of linear amplification at 25 and 37 °C (Figures S3b, S4b, S13, and S14). With increasing concentration of duplex beacons, the quadratic amplification suddenly accelerates. We also found that the maximum reaction rate was obtained at 37 °C for quadratic amplification (Figures S9 and S10), which demonstrates that 37 °C is the optimal temperature for all three enzymes to work best. Temperatures higher than 37 °C destroy the structures of the enzymes and reduce the enzymes' activity.

To investigate the detection limit of this strategy, we measured the fluorescence intensities upon addition of various concentrations of miR-21. When the concentration of miR-21 increased gradually, the intensity of the fluorescence signal rose accordingly (Figures 4a and S17). However, when the concentration of miR-21 was increased further, the fluorescence intensity started to saturate. The plateau phenomenon may be due to the depletion of FAM-modified MBs. The threshold line was calculated by the evaluation of the average response of the control plus 3 times the standard deviation ( $3\sigma$  method).

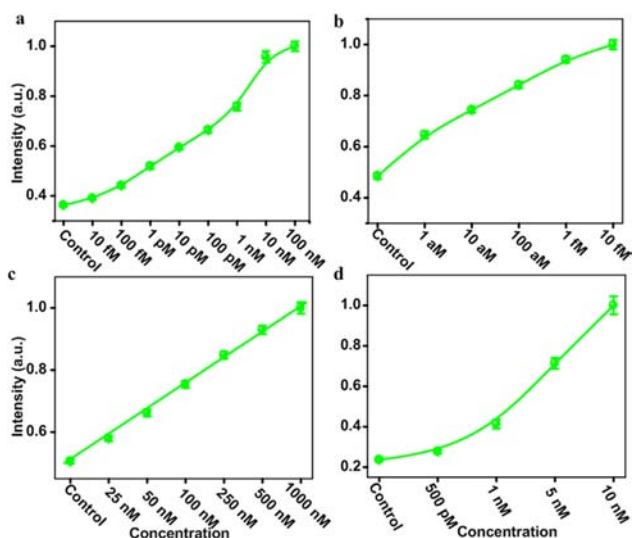


**Figure 4.** Investigation of the sensitivity of (a, b) the HQEA approach at (a) 37 and (b) 4 °C, (c) the traditional MB method, and (d) the Bst polymerase-induced amplification approach. The concentration of probe 21 was 500 nM, and the reaction time was 2 h.

According to this principle, we achieved a detection limit of 10 fM for miR-21 at 37 °C.

Plaxco and co-workers proved that the residual lambda exonuclease activity against unbound MB could be suppressed at 4 °C, thus improving the detection sensitivity.<sup>23</sup> To investigate the ability of the described strategy to quantify the target sensitively, we perform this assay at 4 °C for 50 h. As expected, the fluorescence intensity decreased with decreasing target miRNA concentration (Figures 4b and S18). However, even at a target concentration of 1 aM, an obvious increase in fluorescence relative to the control was observed. For one thing, the background signal was suppressed effectively (Figure S16), and for another, this result also demonstrates that our quadratic amplification has a strong ability to amplify signal. Accordingly, we realized a detection limit of 1 aM at 4 °C, corresponding to nine strands of miR-21 in a 15  $\mu$ L sample.

To assess the amplification function of our quadratic amplification, we also monitored the fluorescence sensitivities of the traditional MB method and the Bst-induced linear amplification reaction and obtained detection limits of 25 nM (Figures 4c and S19) and 500 pM (Figures 4d and S20), respectively. Obviously, the sensitivity of our quadratic amplification for miRNA detection is almost 6 orders of magnitude higher than that of the MB method without any amplification and more than 4 orders of magnitude higher than that of the reported target recycling amplification method (Table S4). These results indicate that our quadratic amplification scheme can ensure an ultrahigh sensitivity for miRNA detection, in accordance with our theoretical analysis (Tables S2 and S3 and Figures S6–S8 and S12).

We then designed a series of experiments to interrogate the specificity of HQEA using miR-21 and miR-221 as targets (Figures 5 and S21–24). To investigate the specificity of HQEA technology for miR-21, we performed a series of contrast experiments using miR-210, miR-221, single-base-mismatched miR-21 (SM miR-21), and three-base-mismatched miR-21 (TM miR-21) as negative controls and a sample without target as a blank control. The results (Figures 5a and S22) showed that the fluorescence signals from miR-210 and

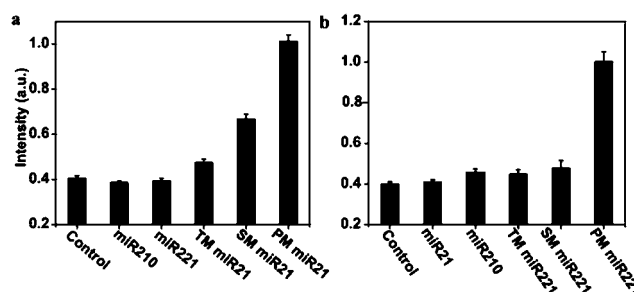


**Figure 5.** Specificity investigations of (a) probe 21 and (b) probe 221. The reaction time was 40 min. Error bars were calculated from three independent experiments.

miR-221 scarcely changed compared with the blank control, while the signals of SM miR-21 and TM miR-21 showed slight increases compared with the blank control. Nevertheless, 10 nM perfectly matched miR-21 (PM miR-21) exhibited a much stronger response than the blank control, which could be easily discriminated from the SM and TM signals. Moreover, when applied in a complex environment (diluted serum), the HQEA method also could discriminate between single-nucleotide polymorphisms efficiently (Figure S25).

To illustrate the generality of our design, we also employed miR-221 to investigate the specificity of the HQEA method (Figures 5b and S23). The only difference between probe 21 and probe 221 is the sequence of the loop region, and therefore, in the design of probe 221, we just needed to replace the loop sequence of probe 21 by that complementary to miR-221. Figure 5b shows that the fluorescence intensities from miR-210, miR-21, SM miR-221, and TM miR-221 all were similar to that of the blank control and far lower than that from PM miR-221. The above results prove that the design of our probe is simple and that theoretically our strategy is suitable for other miRNAs. The universality of our HQEA technology can be realized by altering the loop sequence of the MB probe.

To investigate the feasibility of HQEA to detect miRNAs in complex biological matrices, we first analyzed cell lysate samples from MCF-7 and PC3 cancer cell lines. Figure 6a,b shows the MB fluorescence intensities upon the addition of different numbers of MCF-7 and PC3 cells, respectively. A

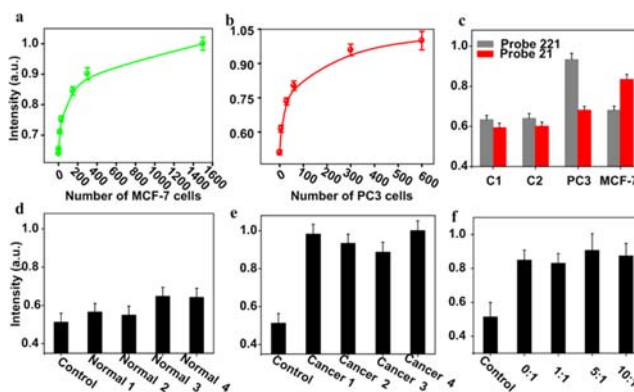


**Figure 6.** (a, b) When this assay was applied to cell lysates, single-cell-level detection limits were obtained for the (a) MCF-7 and (b) PC3 cell lines. (c) Specificity investigation at the cell level for probe 21 and probe 221. C1, sample without any target; C2, sample digested by RNase. (d–f) Fluorescence intensities from (d) four normal samples, (e) four breast cancer samples, and (f) mixtures of normal 2 and cancer 3 samples in ratios of 0:1, 1:1, 5:1, and 10:1.



dramatic increase in the fluorescence intensity was observed as the number of cells increased from one to hundreds. The limit of detection based on the  $3\sigma$  method was approximately a single cell. We next demonstrated the specificity of the approach in cell extracts. Figure 6c shows that miR-21 is expressed in both MCF-7 and PC3 cells, whereas miR-221 is mainly expressed in PC3 cells and barely expressed in MCF-7 cells. These results show that our assay has the potential for application to cell extracts.

Differential expressions of certain miRNA have been shown to be an accurate predictor of a patient's overall prognosis.<sup>26</sup> To investigate the applicability of this approach in clinical diagnosis, we performed this assay on crude extracts of breast cancer tissues (Figures S26–29). Signal intensities from the normal samples were slightly higher than that of the control without RNA extracts (Figure 6d), but those from the cancer samples were significantly higher than those of the control and normal samples (Figure 6e). We then challenged our assays with mixtures of the normal 2 and cancer 3 samples at ratios of 0:1, 1:1, 5:1, and 10:1, and the changes in the fluorescence intensities were not very obvious (Figure 6f). These results demonstrate that our assay holds great promise for cancer diagnosis with great selectivity and accuracy.

In conclusion, we have developed a quadratic amplification strategy based on polymerase-aided strand-displacement polymerization<sup>27–29</sup> and exonuclease-assisted template recycling that achieves rapid, isothermal, and highly sensitive detection of miRNAs extracted from cancer cell lines and clinical samples. Aside from sensitivity (Table S5), our assay requires only one step to realize quadratic amplification for ultrasensitive detection of miRNAs, without the need for multiple self-assembly steps as required in nanoparticle-based amplification assays<sup>14,15</sup> or complicated operations as required in the rolling-circle amplification method.<sup>30,31</sup> The proposed approach should be a promising tool for miRNAs research. For example, the early diagnosis of disease could be realized via quantitative studies of miRNA.

## ■ ASSOCIATED CONTENT

### ● Supporting Information

Experimental procedures and analytical data. This material is available free of charge via the Internet at <http://pubs.acs.org>.

## ■ AUTHOR INFORMATION

### Corresponding Author

xiafan@hust.edu.cn

### Author Contributions

<sup>†</sup>R.D., X.Z., and S.W. contributed equally.

### Notes

The authors declare no competing financial interest.

## ■ ACKNOWLEDGMENTS

This research was supported by initiatory financial support from HUST, the National Basic Research Program of China (973 Program) (2012CB932600, 2012CB933800, 2011CB935700, 2012CB933200, and 2013CB933000), the 100 Talent Project from the Chinese Academy of Sciences (to X.Z.) and the 1000 Young Talent Program (to F.X.), the National Natural Science Foundation of China (21175140, 20974113, and 21121001), and the Key Research Program of the Chinese Academy of Sciences (KJZD-EW-M01).

## ■ REFERENCES

- (1) Lee, R. C.; Feinbaum, R. L.; Ambros, V. *Cell* **1993**, *75*, 843.
- (2) Hutvagner, G.; Zamore, P. D. *Science* **2002**, *297*, 2056.
- (3) Bartel, D. P. *Cell* **2004**, *116*, 281.
- (4) Lagos-Quintana, M.; Rauhut, R.; Lendeckel, W.; Tuschl, T. *Science* **2001**, *294*, 853.
- (5) He, L.; Hannon, G. J. *Nat. Rev. Genet.* **2004**, *5*, 522.
- (6) Válczi, A.; Hornyik, C.; Varga, N.; Burgyón, J.; Kauppinen, S.; Havelda, Z. *Nucleic Acids Res.* **2004**, *32*, No. e175.
- (7) Lee, J.; Cho, H.; Jung, Y. *Angew. Chem., Int. Ed.* **2010**, *49*, 8662.
- (8) Lee, I.; Ajay, S. S.; Chen, H.; Maruyama, A.; Wang, N.; MacInnis, M. G.; Athey, B. D. *Nucleic Acids Res.* **2008**, *36*, No. e27.
- (9) Allawi, H. T.; Dahlberg, J. E.; Olson, S.; Lund, E.; Ma, W. P.; Takova, T.; Neri, B. P. *RNA* **2004**, *10*, 1153.
- (10) Hartig, J. S.; Grüne, I.; Najafi-Shoushtari, S. H.; Famulok, M. *J. Am. Chem. Soc.* **2004**, *126*, 722.
- (11) Chen, C.; Ridzon, D. A.; Broomer, A. J.; Zhou, Z.; Lee, D. H.; Nguyen, J. T.; Barbisin, M.; Xu, N. L.; Mahuvakar, V. R.; Andersen, M. R.; Lao, K. Q.; Livak, K. J.; Guegler, K. J. *Nucleic Acids Res.* **2005**, *33*, No. e179.
- (12) Li, J.; Yao, B.; Huang, H.; Wang, Z.; Sun, C.; Fan, Y.; Chang, Q.; Li, S.; Wang, X.; Xi, J. *Anal. Chem.* **2009**, *81*, 5446.
- (13) Jia, H.; Li, Z.; Liu, C.; Cheng, Y. *Angew. Chem., Int. Ed.* **2010**, *49*, 5498.
- (14) Fang, S.; Lee, H. J.; Wark, A. W.; Corn, R. M. *J. Am. Chem. Soc.* **2006**, *128*, 14044.
- (15) Li, J.; Schachermeyer, S.; Wang, Y.; Yin, Y.; Zhong, W. *Anal. Chem.* **2009**, *81*, 9723.
- (16) Song, S.; Liang, Z.; Zhang, J.; Wang, L.; Li, G.; Fan, C. *Angew. Chem., Int. Ed.* **2009**, *48*, 1.
- (17) Wang, K. M.; Tang, Z. W.; Yang, C. Y. J.; Kim, Y. M.; Fang, X. H.; Li, W.; Wu, Y. R.; Medley, C. D.; Cao, Z. H.; Li, J.; Colon, P.; Lin, H.; Tan, W. H. *Angew. Chem., Int. Ed.* **2009**, *48*, 856.
- (18) Wei, F.; Wang, J.; Liao, W.; Zimmermann, B. G.; Wong, D. T.; Ho, C. M. *Nucleic Acids Res.* **2008**, *36*, No. e65.
- (19) Zhang, X.; Wang, Z.; Xing, H.; Xiang, Y.; Lu, Y. *Anal. Chem.* **2010**, *82*, 5005.
- (20) Li, J.; Chu, Y.; Lee, B. Y. H.; Xie, X. S. *Nucleic Acids Res.* **2008**, *36*, No. e36.
- (21) Kiesling, T.; Cox, K.; Davidson, E. A.; Dretchen, K.; Grater, G.; Hibbard, S.; Lasken, R. S.; Leshin, J.; Skowronski, E.; Danielsen, M. *Nucleic Acids Res.* **2007**, *35*, No. e117.
- (22) Van Ness, J.; Van Ness, L. K.; Galas, D. J. *Proc. Natl. Acad. Sci. U.S.A.* **2003**, *100*, 4504.
- (23) Zuo, X.; Xia, F.; Xiao, Y.; Plaxco, K. W. *J. Am. Chem. Soc.* **2010**, *132*, 1816.
- (24) Freeman, R.; Liu, X.; Willner, I. *Nano Lett.* **2011**, *11*, 4456.
- (25) Zuo, X.; Xia, F.; Patterson, A.; Soh, H. T.; Xiao, Y.; Plaxco, K. W. *ChemBioChem* **2011**, *12*, 2745.
- (26) Esquela-Kerscher, A.; Slack, F. J. *Nat. Rev. Cancer* **2006**, *6*, 259.
- (27) Connolly, A. R.; Trau, M. *Angew. Chem., Int. Ed.* **2010**, *49*, 2720.
- (28) Guo, Q.; Yang, X.; Wang, K.; Tan, W.; Li, W.; Tang, H.; Li, H. *Nucleic Acids Res.* **2009**, *37*, No. e20.
- (29) Walker, G. T.; Little, M. C.; Nadeau, J. G.; Shank, D. D. *Proc. Natl. Acad. Sci. U.S.A.* **1992**, *89*, 392.
- (30) Zhou, Y.; Huang, Q.; Gao, J.; Lu, J.; Shen, X.; Fan, C. *Nucleic Acids Res.* **2010**, *38*, No. e156.
- (31) Cheng, Y.; Zhang, X.; Li, Z.; Jiao, X.; Wang, Y.; Zhang, Y. *Angew. Chem., Int. Ed.* **2009**, *121*, 3318.